Isolated rings of mesoscopic dimensions. Quantum coherence and persistent currents

by Ho-Fai Cheung Yuval Gefen Eberhard K. Riedel

Persistent currents in small nonsuperconducting rings threaded by a magnetic flux are a manifestation of novel quantum effects in submicron systems. We present theoretical results for one-channel and multichannel systems concerning the dependence of the current amplitude on the number of channels and geometry, temperature, and degree of disorder. Inelastic scattering is considered for one-channel loops only. We also discuss the observability of the effect.

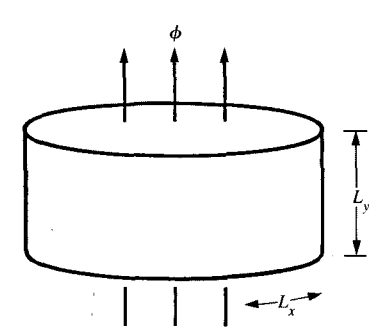
1. Introduction

With the advances in technology, the fabrication of submicron devices has become possible. Such "mesoscopic" systems [1, 2] have opened the door to a rich new field of theoretical and experimental physics. The physics of small metallic rings is an excellent testing ground for many ideas

^eCopyright 1988 by International Business Machines Corporation. Copying in printed form for private use is permitted without payment of royalty provided that (1) each reproduction is done without alteration and (2) the *Journal* reference and IBM copyright notice are included on the first page. The title and abstract, but no other portions, of this paper may be copied or distributed royalty free without further permission by computer-based and other information-service systems. Permission to *republish* any other portion of this paper must be obtained from the Editor.

in the field of mesoscopic physics. The Aharonov-Bohm oscillations in the magnetoresistance of small two- and four-terminal structures have been discussed extensively in the literature [3]. The problem of persistent currents, pertinent to isolated conducting loops or cylinders threaded by a magnetic flux, is less well understood theoretically, and such currents have not yet been observed experimentally. Here we review some recent theoretical progress on that topic.

Persistent currents in nonsuperconducting rings and cylinders threaded by a magnetic flux depend crucially on the coherence of the electron wavefunction over the whole ring [4, 5]. In terms of the phase-coherence length of the electron, L_{\star} (i.e., the length scale over which the electron can be considered to be in a pure state), the requirement is that L_{\star} be larger than the circumference of the rings, L_{\star} . Earlier works in the 1960s, dealing with flux quantization in superconducting rings, mention the possibility of circulating currents in sufficiently small normal-metal rings [6-11]. However, the idea of persistent currents in normal-metal rings containing elastic scatterers is more recent and is based on the observation that the electron wavefunction may even then extend coherently over the whole circumference of the ring. For one-dimensional loops, the existence of such currents was proposed by Büttiker, Imry, and Landauer [4] in 1983, and was extended by Büttiker [5] in 1985. A more



Thin hollow cylinder of circumference $L_{\rm x}$ and height $L_{\rm y}$ threaded by a magnetic flux ϕ .

detailed quantitative analysis has since been given by us [12]. Basic questions concerning the more realistic multichannel systems remained unresolved: most importantly, the dependence of the persistent current on the number of channels, on temperature, and on the amount of elastic scattering (due to impurities and imperfections).

The purpose of the present paper is to review some of our findings for the persistent current in one-channel and multichannel rings. We emphasize the effects of geometry (i.e., number of channels) and temperature. Predictions for the amplitude of persistent currents in experiments require further elucidation of the effects of impurities and will be published elsewhere. We have organized the material as follows. In Section 2, we discuss the effects of geometry on the persistent current in rings at zero temperature and in the absence of disorder. In Section 3, we evaluate the temperature dependence of the current amplitude, and in Section 4 we consider the reduction of the persistent current due to dephasing by inelastic scattering. In Section 5, we comment on the effects of disorder on the persistent current. Section 6 contains a brief summary of our conclusions concerning the observability of the effect. In the remainder of this introduction, we define the persistent current problem in more detail.

We consider the persistent current in multichannel systems of cylinder geometry (Figure 1). The circumference and height of the cylinder are denoted by L_x and L_y or the dimensionless quantities L and M, to be specified later. M is referred to as the number of channels. (We neglect the width of the cylinder, assuming L_z smaller or of the order of the Fermi wavelength of the electron. The generalization to finite L_z is straightforward.) We assume that the magnetic flux ϕ threads the cylinder axially so that the electrons

always move in a field-free space. The flux periodicity of the electron wavefunction, with period $\phi_0 = hc/e$, is then strictly of the Aharonov-Bohm type. We also assume that the selfinductance of the rings is small, so that self-inductance corrections to the flux may be neglected. This is supported by quantitative estimates based on realistic values for the size of the system [13]. For the ring geometry, the spatial degrees of freedom of the electrons are the azimuthal angle θ and the height coordinate y. We replace θ with $x = L\theta/2\pi$, which varies between 0 and L. The vector potential \vec{A} may be chosen to have the form $\vec{A} = 2\pi r \hat{\theta} \phi / L^2$, where ϕ is the flux through the cylinder, r the radial distance, and $\hat{\theta}$ the azimuthal unit vector. We apply periodic boundary conditions in the azimuthal direction and hard-wall ones in the y-direction. The current I_n carried by the nth eigenstate (of energy E_n) may be calculated by using the current operator. Instead, we work in a gauge for the vector potential in which the field does not appear explicitly in the Hamiltonian and the current operators, but enters the calculation via the flux-modified azimuthal boundary conditions [6, 11],

$$\psi(L) = \exp\left(\frac{i2\pi\phi}{\phi_0}\right)\psi(0),$$

$$\frac{d\psi}{dx}\Big|_{L} = \exp\left(\frac{i2\pi\phi}{\phi_0}\right)\frac{d\psi}{dx}\Big|_{0},$$
(1)

where $\phi_0 = hc/e$. These equations imply that the eigenstates and energies and hence all equilibrium physical properties of the ring are periodic in ϕ with period ϕ_0 . This is true also in the presence of disorder. A flux $\phi \neq \phi_0 \times$ integer is mathematically equivalent to a change in the boundary conditions of the system. This observation is the key to all our discussions of the sensitivity of the persistent current to changes in temperature, degree of disorder, and other parameters.

The total current, $I(\phi)$, is the sum over the contributions I_n of all states, weighted with the appropriate occupation probability. It is periodic in ϕ/ϕ_0 , with period 1, and can be expressed as a Fourier sum,

$$I(\phi) = \sum_{l=1}^{\infty} A_l \sin\left(\frac{2l\pi\phi}{\phi_0}\right). \tag{2}$$

To calculate the persistent current we need to know the eigenstates of the system and the thermal distribution function. Typical for mesoscopic systems is the fact that the energy levels form a discrete spectrum. In principle, the canonical and grand-canonical ensembles give rise to different single-level probability distributions, because the systems are not in the thermodynamic limit. For a ring, which can exchange energy with a reservoir, a description in terms of a canonical ensemble with fixed number of particles N_e is appropriate. It is more convenient to consider a system that also couples weakly to a particle reservoir (cf. also Section 2). Adapting this approach, we characterize the

system by a Fermi-Dirac distribution with the chemical potential μ , and compute the persistent current at finite temperatures starting from

$$I(\phi) = \sum_{n} \frac{1}{e^{\beta(E_{n}-\mu)} + 1} I_{n}.$$
 (3)

 I_n and E_n denote the energy and current of the *n*th eigenstate, $\beta = 1/k_B T$.

There is a close connection between the states of an electron in a loop and the one-dimensional Bloch problem, as seen by identifying $2\pi\phi/\phi_0$ and kL_x [4, 6, 11]. The energy levels of the ring form microbands as a function of ϕ with period ϕ_0 analogous to the Bloch electron bands in the extended k-zone picture (cf. Figure 2). The current carried by level E_x at T=0 is

$$I_n = -\frac{ev_n}{L_x}, \qquad v_n = \frac{1}{\hbar} \frac{\partial E_n}{\partial k_n}, \tag{4}$$

or, using the above analogy,

$$I_n = -c \frac{\partial E_n}{\partial \phi}. ag{5}$$

At finite temperatures, instead of summing the currents I_n over all levels with weight $f(E_n)$, one can calculate the total current from the thermodynamic potential, F, of the system [6, 11],

$$I(\phi) = -c \frac{\partial F}{\partial \phi}.$$
 (6)

Figure 2 shows schematically the energies of the eigenstates of three small cylinders of different circumference to height ratios as a function of flux. In the presence of disorder, gaps open at the points of intersection, in the same way as band gaps form in the band structure problem. From Equation (5), the current carried by an eigenstate is proportional to the slope of the energy-versus-flux curve.

2. Persistent current in perfect rings

First, we consider persistent currents in perfect rings at zero temperature and vanishing disorder as a function of geometry. These results provide the background against which we discuss the effects of temperature and disorder. Our calculations are for noninteracting systems of electrons. We concentrate on the generic results as obtained from the free-electron and tight-binding models.

The free-electron model of the cylinder is defined by

$$H = -\frac{\hbar^2}{2m} \left(\frac{d^2}{dx^2} + \frac{d^2}{dy^2} \right) + V(x, y), \tag{7}$$

with the boundary conditions (1). For the perfect cylinder, V = 0, the energy and current of the (n, m)th eigenstate are

$$E_{n,m} = \frac{\hbar^2}{2m} [k_x^2(n,\phi) + k_y^2(m)],$$

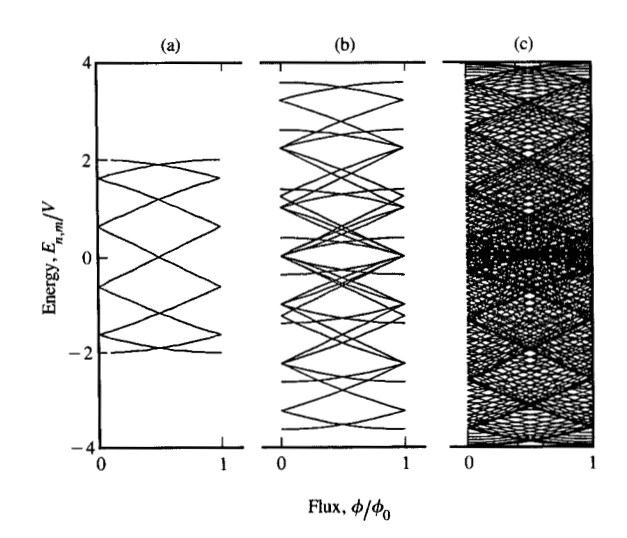


Figure 2

Energy levels as a function of flux for the tight-binding model (14) of cylinders of size (a) 10×1 , (b) 10×4 , and (c) 10×40 . Results are for rings without disorder.

$$I_{n,m} = -\frac{e\hbar}{mL} k_x(n,\phi),\tag{8}$$

where $k_x(n, \phi) = 2\pi [n + (\phi/\phi_0)]/L_x$, $k_y(m) = m\pi/L_y$, with $n = 0, \pm 1, \pm 2, \cdots$ and $m = 1, 2, 3, \cdots$. The system is characterized by the chemical potential $\mu = \hbar^2 k_F^2/2m$. One can visualize the effect of nonzero flux as a shift of the (k_x, k_y) grid in the k_x -direction relative to the fixed Fermi half-sphere, $k_F^2 = k_x^2 + k_y^2$ with $k_y > 0$; see Figure 3(a). In units of the Fermi wavelength $\lambda_F = 2\pi/k_F$, the circumference and height of the cylinder are $L = L_x/\lambda_F$ and $\tilde{L}_y = L_y/\lambda_F$. The number of channels M is defined as the largest integer $\leq 2\tilde{L}_y$, i.e., the largest channel index inside the Fermi surface. We denote by Δ_M the level spacing at the Fermi surface for zero flux. For the one-channel system,

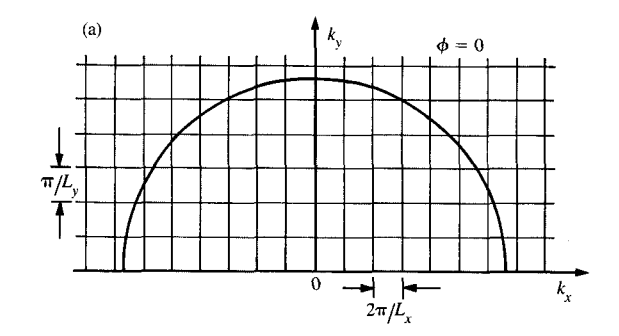
$$\Delta_{\rm l} = \frac{2\pi\hbar v_{\rm F}}{L_{\star}};\tag{9}$$

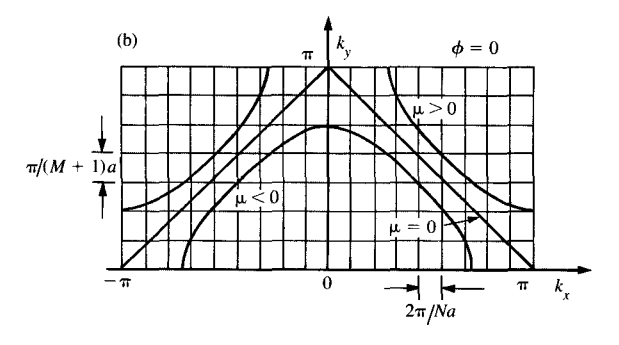
there are two eigenstates per energy interval Δ_1 . Δ_M scales like Δ_1/M .

The total persistent current may be expressed as the sum over the currents carried by the M different channels. For the one-channel problem we had obtained [12]

$$I_1(\phi) = \sum_{l=1}^{\infty} \frac{2I_0}{\pi l} \cos(lk_{\rm F}L_x) \sin\left(\frac{2l\pi\phi}{\phi_0}\right),\tag{10}$$

with $I_0 = ev_F/L_x$. For the *M*-channel system, the total current $I_M(\phi)$ may be obtained by summing over all channels k_v , with their respective $k_F(k_v) = \sqrt{k_F^2 - k_v^2}$,





Elamak.

Fermi surfaces and eigenstates at zero flux in (k_x, k_y) space for (a) free-electron model (7) and (b) tight-binding model (14) of perfect cylinders of circumference and height L_x , L_y , and $L_x = Na$, $L_y = Ma$, respectively (a = lattice constant).

$$I_{M}(\phi) = \sum_{m=1}^{M} \sum_{l=1}^{\infty} \frac{2I_{0}\sqrt{1 - [k_{y}(m)/k_{F}]^{2}}}{\pi l} \cdot \cos\{lk_{F}L_{x}\sqrt{1 - [k_{y}(m)/k_{F}]^{2}}\}\sin\left(\frac{2l\pi\phi}{\phi_{0}}\right).$$
(11)

Analytical results for $I_M(\phi)$ can easily be obtained in the limits of long cylinders $(L_x \ll L_y)$ and short cylinders $(L_x \gg L_y)$, respectively. The result of the summation over m in Equation (11) depends on the strength of the phase correlations between currents of different channels, as described by the cosine phase factor. For the long cylinder, $L_x \ll L_y$, that cosine phase factor changes slowly with k_y . Replacing the sum with an integral, we obtain

$$I_{M}(\phi) = \sum_{l=1}^{\infty} \frac{MI_{0}}{\pi l \sqrt{lL}} \cos\left(lk_{F}L_{x} - \frac{\pi}{4}\right) \sin\left(\frac{2l\pi\phi}{\phi_{0}}\right). \tag{12}$$

For the short cylinder, $L_x \gg L_y$, the cosine phase factor in Equation (11) changes rapidly with k_y . Consequently, the actual form of the current depends sensitively on L_x , L_y , and k_F . To estimate its typical magnitude we assume the cosine phase factors in Equation (11) to be completely uncorrelated

for different k_y . (This assumption agrees well with our numerical results.) The typical current is then $\overline{I}_M(\phi) = \sqrt{\langle I_M^2(\phi) \rangle}$, where

$$\langle I_M^2(\phi)\rangle = \sum_{l=1}^{\infty} \langle A_l^2 \rangle \sin^2\left(\frac{2l\pi\phi}{\phi_0}\right),$$
 (13a)

witl

$$\sqrt{\langle A_l^2 \rangle} = \frac{2I_0}{\pi l} \sqrt{\frac{M}{3}}.$$
 (13b)

The formulas (10)–(13) contain important physics, which is discussed below.

The current-flux characteristics $I_1(\phi)$ for one-dimensional loops, cf. Equation (10), are shown in **Figure 4** for three choices of μ (or $k_{\rm F}$) [14]. For $k_{\rm F}=N_{\rm e}\pi/L_{\rm x}$, the loop has a fixed number of electrons $N_{\rm e}$ (even or odd), while for other $k_{\rm F}$ the number of electrons varies when the flux ϕ is changed by one fluxoid. Whenever a level crosses the Fermi surface, a sawtooth change occurs in the current-flux characteristic. The maximum current amplitude is inversely proportional to the loop circumference, $I_0=ev_{\rm F}/L_x$. In one dimension, the total current has the same sign and order of magnitude as the current of the highest occupied level.

The current-flux characteristics $I_M(\phi)$ for M-channel cylinders may be thought of as a superposition of M sawtooth-shaped currents $I_1(\phi)$ corresponding to different $k_{\rm F}(k_{\rm w})$, as expressed by Equation (11). In Figure 3, the mth channel corresponds to all states inside the Fermi surface with fixed $k_{\nu}(m) \le k_{\rm F}$. For short cylinders, $L_{\nu} \gg L_{\nu}$, there is apparently no correlation between the separations of the last occupied level and the Fermi energy from channel to channel, so that the channel currents add without phase correlation. Therefore, the total current amplitude scales with the number of channels like \sqrt{M} , as was obtained in Equation (13b). We note that in spite of the strong cancellations, the typical total current increases with the number of channels. For long cylinders, $L_{\nu} \ll L_{\nu}$, there are some phase correlations among the currents associated with different channels (and eigenstates). This is also seen from the level diagram of Figure 2(c). The analytical result (12) shows that in this case the total current scales with M like M/\sqrt{L} . Note that in both cases the unit of current is $I_0 = ev_F/L_x$, which also depends on L_x . In Figures 9 and 10, the curves labeled $T/T^* = 0$ are representative current-flux characteristics for a single long and a single short cylinder, respectively [14]. Figures 9 and 10 are discussed in more detail in Section 3.

The tight-binding model for a cylinder of circumference $L_v = Na$ and height $L_v = Ma$ is defined by

$$H = -V \sum_{i,j} (a_{i,j}^{\dagger} a_{i+1,j} + a_{i+1,j}^{\dagger} a_{i,j} + a_{i,j}^{\dagger} a_{i,j+1} + a_{i,j+1}^{\dagger} a_{i,j})$$

$$+ \sum_{i,j} \epsilon_{i,j} a_{i,j}^{\dagger} a_{i,j}$$
(14)

and the boundary conditions (1). Here $a_{i,j}^{\dagger}$ and $a_{i,j}$ denote the creation and annihilation operators at site (i,j), V the hopping matrix element, $\epsilon_{i,j}$ the on-site energy, and a the lattice constant. For the perfect cylinder, $\epsilon_{i,j} \equiv 0$, the eigenstates are

$$\psi(x,y) = \sqrt{\frac{2}{N(M+1)}} e^{ik_x x} \sin k_y y, \tag{15}$$

where both x and y are discrete, and k_x and k_y are

$$k_{x} \equiv k_{x}(n, \phi) = \frac{2\pi}{N} \left(n + \frac{\phi}{\phi_{0}} \right), \tag{16}$$

$$k_{y} \equiv k_{y}(m) = \frac{m\pi}{M+1},$$

with $n = 0, 1, \dots, N-1$ and $m = 1, 2, \dots, M$. The energy and current of the eigenstate (n, m) are

$$E_{n,m} = -2V(\cos k_x a + \cos k_y a),$$

$$I_{n,m} = -\frac{4\pi cV}{N\phi_0} \sin k_x a.$$
(17)

For the one-dimensional loop, the level spacing at the Fermi surface at zero flux is

$$\Delta_{\rm l} = \frac{4\pi V}{N} \sin k_{\rm F} a,\tag{18}$$

which has the same form as Equation (9). For the two-dimensional cylinder described by the tight-binding model, the level spacing Δ_M scales like 1/M, except at $\mu=0$, where it scales as $1/M\log M$. The Fermi surface consists of two straight lines [see Figure 3(b)]; the states with $E_{n,m}<0$ are located inside the triangle.

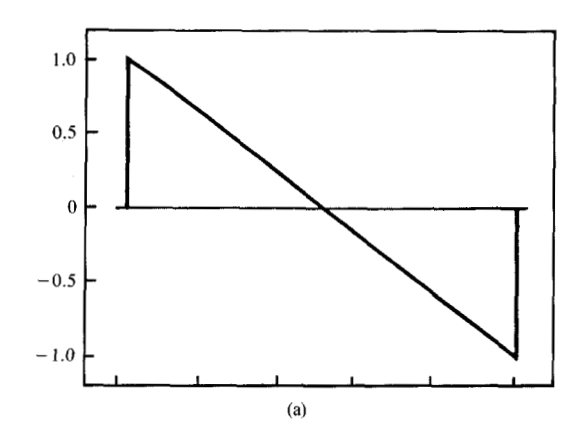
For the tight-binding model with M = 1 we had obtained [12]

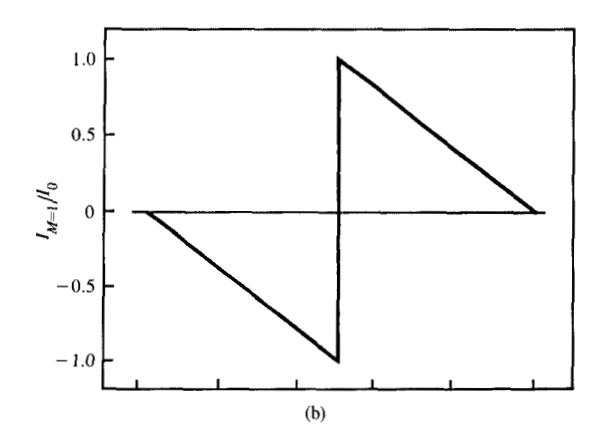
$$I_1(\phi) \approx \sum_{l=1}^{\infty} \frac{2I_0}{\pi l} \cos(lNk_{\rm F}a) \sin\left(\frac{2l\pi\phi}{\phi_0}\right),$$
 (19)

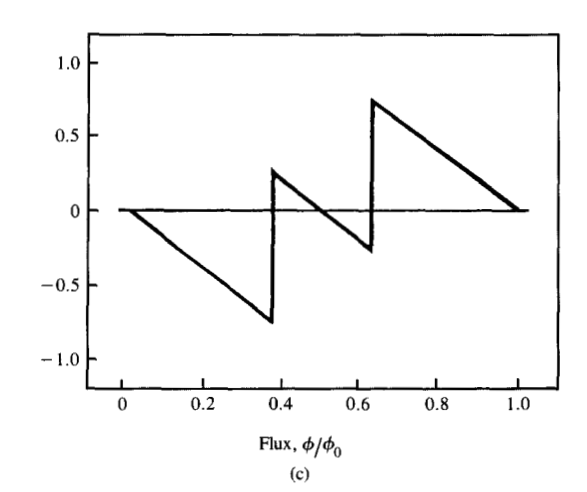
which is similar to Equation (10) for the free-electron model. The $I-\phi$ characteristics are also very similar to those of Figure 4. As expected, now $I_0 = (2eV/Nh)\sin k_{\rm F}a$ vanishes for filled bands, where $k_{\rm F}a = \pi$.

The total persistent current $I_M(\phi)$ of the M-channel system may be expressed as the sum of the currents over the M channels, each with a contribution given by Equation (19), with $k_F(k_y)$. Except for the half-filled band limit, $\mu=0$, it exhibits the same generic features as Equations (12) and (13). (Compare also the discussion of Figure 7, shown later.) In the following, we specialize to the half-filled band case to illuminate the working of the phase correlations described by the cosine phase factor in Equation (19).

For the two-dimensional tight-binding model in the halffilled band limit, the total persistent current is







Persistent current vs. flux $(I-\phi)$ characteristics of perfect one-channel loops over one period of the magnetic flux ϕ/ϕ_0 , cf. Equation (10) [14]. The chemical potential μ is fixed such that the number of states with energy less than μ in the loop is (a) even, (b) odd, and (c) changes between odd and even as a function of the flux. The current is in units of $I_0 = ev_F/L_x$. Results for the one-channel tight-binding model are very similar.

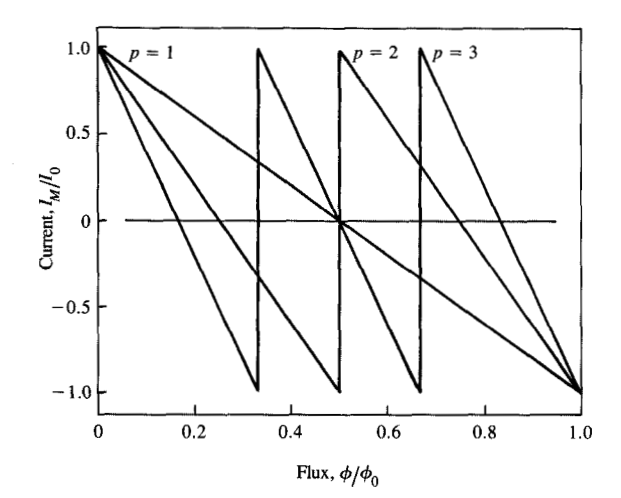


Figure 9

Effect of interchannel phase correlations of the $I-\phi$ characteristics of M-channel cylinders described by the tight-binding model in the half-filled band limit $\mu=0$ [cf. Equation (20)]. N and M satisfy the phase-correlation condition (21) for p=1, 2, and 3, respectively, at j=1. The l=1, 2, and 3 harmonics dominate in the respective persistent currents, and the maximum possible amplitude, $I_{\text{max}}=2(M+1)I_0/\pi p$, is achieved. The curves are general, though they were generated for sample sizes 100×49 , 100×99 , and 100×149

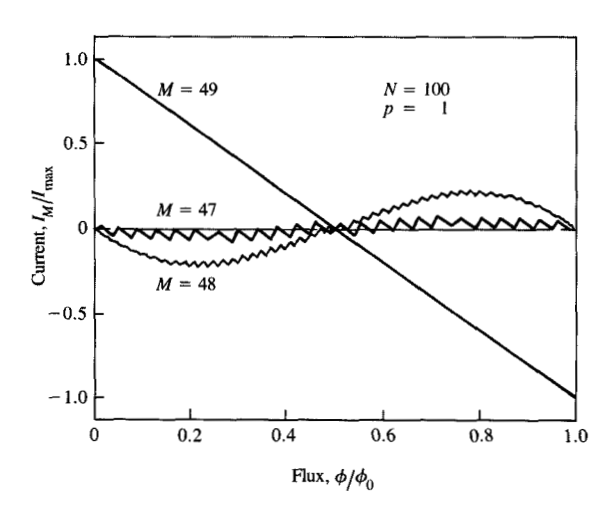


Figure 6

Sensitivity of the $I-\phi$ characteristics (p=1) of M-channel cylinders considered in Figure 5 to the degree to which N and M satisfy the phase-correlation condition (21). For $\delta M=1$ and 2 (and j=1), the amplitude of the dominant first harmonic is reduced by factors of 1/3 and 1/15, respectively.

$$I_{M}(\phi) = \sum_{l=1}^{\infty} \frac{2I_{0}}{\pi l} \cos^{2}\left(\frac{lN\pi}{2}\right)$$

$$\cdot \frac{\sin\left(\frac{\pi}{M+1}\right)}{\cos\left(\frac{lN\pi}{M+1}\right) - \cos\left(\frac{\pi}{M+1}\right)} \sin\left(\frac{2l\pi\phi}{\phi_{0}}\right). \tag{20}$$

The current is largest when strong phase correlations exist between the currents from channel to channel. Consider Figure 3(b). Changing the flux ϕ means moving the underlying (k_x, k_y) grid in the k_x -direction relative to the triangular Fermi surface. Suppose $\Delta k_x = \Delta k_y$; i.e., N =2(M + 1); then the Fermi surface crosses M levels simultaneously while the flux ϕ is changed by one fluxoid. There is perfect phase correlation among the channel currents, and the amplitude of the total current assumes its greatest possible value, $I_{\text{max}} = 2(M+1)I_0/\pi p$. The corresponding $I-\phi$ characteristic is labeled p=1 in Figure 5 [14]. Now suppose $\Delta k_x = p\Delta k_y$; i.e., N = 2(M+1)/p. If we choose M at fixed N (e.g., N = 100) such that the latter condition is satisfied, then the Fermi surface crosses p times a group of M levels while the flux ϕ is changed by one fluxoid. The amplitude of the total current is the same as for the p = 1 case, but now the current changes sign p times within one period ϕ_0 . Figure 5 shows the $I-\phi$ characteristics for p = 1, 2, and 3. The general condition for maximal interchannel phase correlations is

$$N = \frac{2j}{p} (M+1), \tag{21}$$

where p and j are integers that are relatively prime. When this geometrical condition relating the circumference and height of the cylinder is satisfied, then the l=p Fourier coefficient in Equation (20) assumes a maximum and dominates the sum.

Unfortunately, the geometrical amplification of the persistent current described above may not be of much practical use because (a) $\mu=0$ is very special and (b) the geometrical condition (21) is very sharp. For instance, if $N=2j(M+1+\delta M)/p$, so that M differs from the value that satisfies (21) by δM , then the dominant (l=p) Fourier coefficient decreases as $1/[1-(2j\delta M)^2]$. Figure 6 shows this feature. Here, for p=1, j=1, changing M by 1 or 2 relative to the value satisfying (21) reduces the amplitude of the first harmonic of the current by factors of 1/3 and 1/15, respectively. The dependence on the chemical potential μ of the persistent current for a cylinder satisfying the geometrical condition (21) is

$$I_{M}(\phi) = \sum_{n=1}^{\infty} \frac{I_{\text{max}}}{n\pi} \sqrt{\frac{\Delta}{np \mid \mu \mid}} \cdot \cos\left(\frac{2np\pi \mid \mu \mid}{\Delta} + \frac{\pi}{4}\right) \sin\left(\frac{2np\pi\phi}{\phi_{0}}\right). \tag{22}$$

This formula is valid for $|\mu| \ge \Delta_1$. The form of the equation is similar to that of Equation (12), as one would expect, since in both cases there are strong phase correlations among the currents from different channels. **Figure 7** shows results for the $I-\phi$ characteristic, p=1, j=1, for four values of μ . For large $|\mu|$, the Fermi surface approaches a semicircle. Then these results cross over to the results for the free-electron model.

3. Persistent current at finite temperatures

We now discuss the effect of temperature on the persistent current of impurity-free rings. With increasing temperature, the probability that electrons occupy higher levels, which may carry larger currents, increases. However, at higher temperatures, the occupation probabilities of levels close in energy (which encompass levels having currents of opposite sign) are not very different. The net result is an almost complete cancellation of positive and negative contributions to the current. Significant for the observability of the persistent current, we find that even for multichannel rings the sensitivity of the current amplitude to temperature is governed by the level spacing of the one-channel ring, $\Delta_{i,j}$ rather than the much smaller level spacing of the multichannel ring, $\Delta_M \propto \Delta_1/M$. The reason is that there are correlations in the slopes of the eigenenergies as functions of flux.

Finite temperature affects the system in another important way. At nonzero temperature, thermal excitations, such as phonons, are present. Such excitations interact with the electrons inelastically, giving rise to phase randomization of the electron wavefunction (besides some level shifting). The effects of dephasing on the persistent current through inelastic scattering are discussed in the next section. Here we assume that at the temperatures considered, the phase-coherence length of the electron is large compared to the ring circumference, $L_{\rm A}\gg L_{\rm r}$.

We compute the persistent current at finite temperatures starting from Equation (3). We discuss only the case of metallic electron densities, $\mu \gg k_{\rm B}T$. (The Appendix of [12] contains some discussion of other cases and calculational details for one-dimensional rings.) For the one-channel loop in the metallic limit, the persistent current is given by

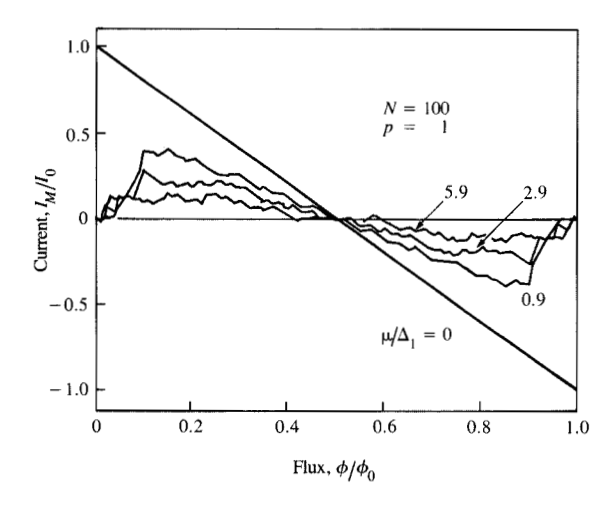
$$I_{1}(\phi) = \sum_{l=1}^{\infty} \frac{4I_{0}T}{\pi T^{*}} \frac{\exp(-lT/T^{*})}{1 - \exp(-2lT/T^{*})}$$

$$\cdot \cos(lk_{F}L_{x})\sin\left(\frac{2l\pi\phi}{\phi_{0}}\right), \tag{23}$$

where

$$k_{\rm B}T^* = \frac{\Delta_1}{2\pi^2}.\tag{24}$$

This result holds both for the free-electron and the tightbinding model, and replaces Equations (10) and (19),



STATITE OF

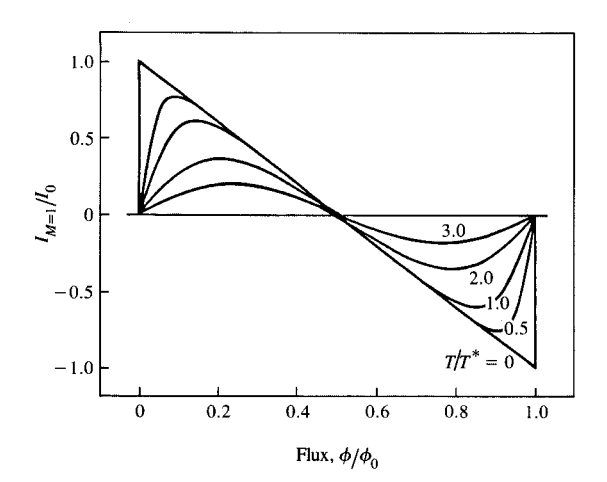
Sensitivity of the $I-\phi$ characteristics (p=1) of M-channel cylinders considered in Figure 5 to changes in the chemical potential. The set of chemical potentials $\mu/\Delta_1=0,0.9,2.9$, and 5.9 was chosen such that the respective currents remain dominated by the first harmonic.

respectively. The characteristic temperature T^* is set by the level spacing $\Delta_1 \propto 1/L_x$ at the Fermi surface [Equations (9) and (18)]. At $T > T^*$, the persistent current is proportional to $\sin(2\pi\phi/\phi_0)$ with an amplitude that decreases exponentially with temperature. For $T < T^*$, higher harmonics contribute and the amplitude of the total current depends only weakly on temperature. These effects are seen in Figure 8. Nonzero temperature has two main effects: All discontinuities in the $I-\phi$ characteristic become rounded, and the maximum amplitude of the current decreases exponentially.

In view of the preceding discussion, one might expect that for M-channel systems the characteristic temperature separating high- and low-temperature regimes is set by the level spacing Δ_M , which is smaller than Δ_1 by a factor of 1/M. That would be devastating for the observability of persistent current effects. However, as discussed subsequently, this is not the case.

Analytical expressions for the persistent current of M-channel cylinders at finite temperature are obtained by following the same procedure as described in Section 2. Starting from Equation (3), we first perform the sum over the states within a single channel, which yields Equation (23), now with $k_{\rm F}$ and T^* depending on $k_{\rm F}$, and then perform the sum over the M single-channel contributions. For the free-electron model, specialized to the limit of long cylinders, we obtain for $T > T^*$





Temperature dependence of the $I-\phi$ characteristics of one-channel loops from the tight-binding model [cf. Equation (23)]. The results are for even numbers of electrons in the loop (see Figure 4) and temperatures $T/T^* = 0$, 0.5, 1.0, 2.0, and 3.0. The characteristic temperature T^* is given by the level spacing at the Fermi surface at zero flux, $T^* = \Delta_1/2\pi^2$. Results for the one-channel free-electron model are similar.

$$\begin{split} I_{M}(\phi) &= \sum_{l=1}^{\infty} \frac{2MI_{0}T}{\pi T^{*}\sqrt{lL}} \exp\left(-\frac{lT}{T^{*}}\right) \\ &\cdot \cos\left(lk_{F}L_{x} - \frac{\pi}{4}\right) \sin\left(\frac{2l\pi\phi}{\phi_{0}}\right). \end{split} \tag{25}$$

For long cylinders, the cosine phase factor in the current [cf. Equation (23)] varies slowly from channel to channel, so that the sum over channels can be replaced by an integral. It is precisely due to these strong correlations in the phase that the total current $I_M(\phi)$ has the characteristic factor of M/\sqrt{L} , as in the T=0 case [cf. Equation (12)]. For short cylinders the cosine phase factor in Equation (23) varies greatly from channel to channel. We estimate the typical amplitude of the lth harmonics $\sqrt{\langle A_l^2 \rangle}$. Assuming that the cosine phase factors are completely uncorrelated for different k_y , we obtain for $T>T^*$

$$\overline{A}_{l} = \sqrt{\langle A_{l}^{2} \rangle} = \frac{2I_{0}\sqrt{M}}{l} \left(\frac{lT}{\pi T^{*}}\right)^{3/4} \exp\left(-\frac{lT}{T^{*}}\right). \tag{26}$$

For $T > T^*$, the first harmonic represents very well the amplitude of the total current. Again, as in the T = 0 case [Equation (13)], the typical total current has the characteristic factor of \sqrt{M} due to the sum over uncorrelated contributions from different channels.

For both long and short cylinders, we see from Equations (25) and (26) that the decrease of the persistent current is

governed by T^* , which is in turn proportional to the level spacing of a one-channel ring of the same circumference, Δ_1 . This is extremely relevant to the observability of the persistent current, since if the decrease were governed by Δ_M , persistent currents would show in experiments only at hopelessly low temperatures. One other general feature that we see from Equations (23), (25), and (26) is that the higher harmonics decrease exponentially more rapidly than the first harmonic, so that at $T > T^*$, the total current is well represented by the first harmonic. Numerical results confirm this behavior.

Numerical results for $I_M(\phi)$ for a long and a short cylinder are shown in **Figures 9 and 10**, respectively [14]. In both cases, they show clearly the total current approaching sinusoidal behavior with increasing temperature.

For the tight-binding model, we discuss the temperature behavior only for the persistent current of cylinders that satisfy the condition of maximal interchannel phase correlation [Equation (21)]. The calculation is the same as for the free-electron model, the one-channel result being given by Equation (23). Summing up the contributions from all channels, we obtain for $T > T^*$

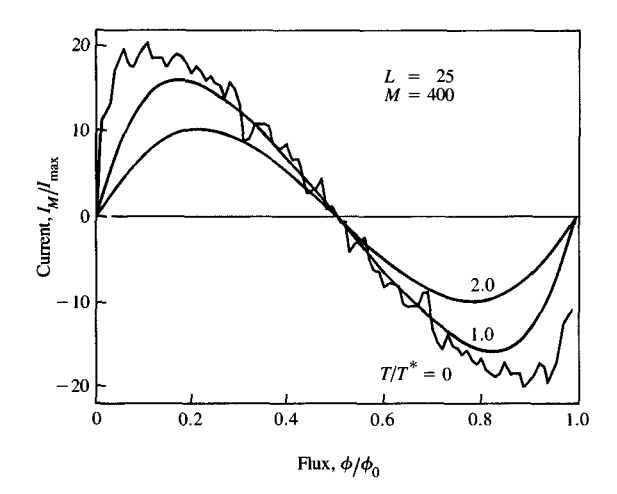
$$I_{M}(\phi) = \sum_{n=1}^{\infty} \frac{2I_{\text{max}}}{n\pi} \sqrt{\frac{npT}{T^{*}}} \sin\left(\frac{2np\pi\phi}{\phi_{0}}\right) \exp\left(-\frac{npT}{T^{*}}\right). \tag{27}$$

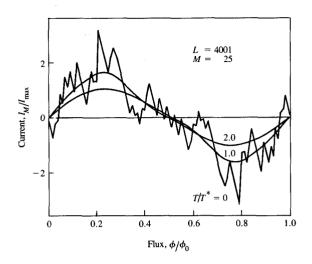
The total current is proportional to the same characteristic factor $I_{\rm max}=2(M+1)I_0/\pi p$, as at T=0, the reason being the complete phase correlation between the currents from different channels. Again, as for the free-electron model, the decrease of the persistent current is governed by Δ_1 , and higher harmonics decrease exponentially faster than the first harmonic.

In this section we have discussed the average persistent current for a ring in thermal equilibrium. By assuming a Fermi-Dirac distribution function for the electrons, we find that the decrease of the current is governed by the level spacing for a one-channel ring, instead of the much smaller level spacing for an M-channel ring. This allays one fear, namely, that the temperature required to observe the persistent current might be vanishingly small. We also find that in general, the first harmonic decreases most slowly and dominates the current at high temperatures, $T > T^*$.

4. Persistent current and phase breaking

Understanding the role of inelastic scattering events that lead to a dephasing of the electron wavefunction is crucial for developing a complete theory of persistent currents; cf. also [4, 5]. Such an understanding is still lacking. To gain some insight into this aspect of the problem, we have considered a phenomenological description of a one-dimensional ring, which follows closely an approach put forward by Büttiker [5]. Büttiker considered a one-dimensional ring coupled through a single ideal lead to an external electron reservoir





Temperature dependence of the $I-\phi$ characteristics of M-channel cylinders from the free-electron model for a long cylinder [14], with L=25 and M=400. Also for M-channel cylinders, the characteristic temperature is $T^*=\Delta_1/2\pi^2$ (i.e., is determined by the level spacing Δ_1 of the single-channel system of the same circumference L_y).

in which thermal equilibration takes place; see Figure 11(a). He cast the coupling to the outside reservoir in the form of a scattering problem, describing the scattering at the junction between the ring and the lead in terms of a (3×3) S-matrix. However, in Büttiker's formulation the scattering of the electron contains both elastic and inelastic contributions, and it is difficult to separate the effects that result from these two very different types of scattering.

We have modified the S-matrix that Büttiker [5, 15] used so that it describes only the inelastic scattering in the ring. This matrix relates the outgoing waves α_1 , β_1 , γ_1 to the incoming waves α , β , γ [see Figure 11(a)] and is written as

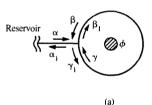
$$\mathbf{S} = \begin{bmatrix} -\sqrt{1 - 2\varepsilon} & \sqrt{\epsilon} & \sqrt{\epsilon} \\ \sqrt{\epsilon} & 0 & \sqrt{1 - \epsilon} \\ \sqrt{\epsilon} & \sqrt{1 - \varepsilon} & 0 \end{bmatrix}. \tag{28}$$

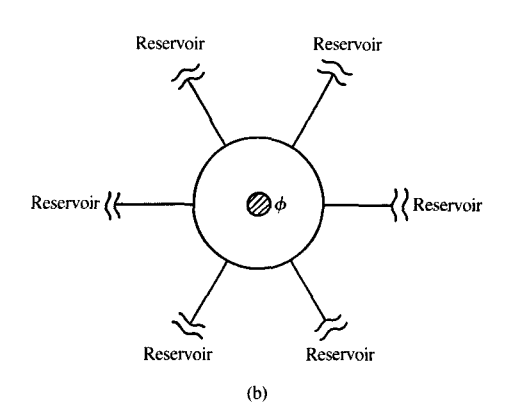
According to this scattering matrix, a particle coming from the reservoir is scattered back with a probability $1-2\epsilon$, and can enter the ring with equal probability, ϵ , for going clockwise or anticlockwise. A particle in the ring arriving at the junction can either scatter out of the ring (with probability ϵ) or remain in the ring (with probability $1-\epsilon$), its momentum being unchanged. No elastic scattering (i.e., backscattering) within the ring is allowed.

The way we have formulated the problem is not absolutely correct, since the S-matrix in Equation (28) is not unitary,

Figure 10

Temperature dependence of the $I-\phi$ characteristics of M-channel cylinders from the free-electron model for a short cylinder [14], with L=4001 and M=25. The characteristic temperature T^* is defined as in Figure 9.





Ring coupled by ideal conductors to (a) one and (b) many external electron reservoirs.

which implies nonconservation of current. When there is only one incoming wave, the current is conserved. It is the interference terms that cause current nonconservation. It may seem that this model is too awkward to have a sound physical meaning. However, remembering that we are modeling inelastic scattering which causes dephasing of the electron wavefunction, we should add an uncontrolled, random phase to the wave after every inelastic scattering event. This means that five of the elements of the S-matrix, the $-\sqrt{1-2\epsilon}$ and $\sqrt{\epsilon}$ terms in Equation (28), should carry extra random phase factors. While these phase factors do not affect any of our discussions below, averaging over these phases restores current conservation. It is important that the two $\sqrt{1-\epsilon}$ elements of the S-matrix not be modified by random phase factors, since they represent the parts of the wavefunction that are not scattered.

The persistent current in the ring can be calculated now, following [5]. With a flux present, the wavefunction satisfies the boundary condition (1). The current is then given [10] by

$$I_{1}(\phi) = -\int ev(E)(|\beta|^{2} - |\gamma|^{2})f(E) \frac{dE}{2\pi\hbar\nu(E)},$$
 (29)

where f(E) denotes the Fermi-Dirac distribution function. We choose the Fermi energy such that there is an odd number of electrons in the ring, when $\epsilon=0$ and T=0. We find for T=0 and ϕ/ϕ_0 (mod 1) in the interval $-0.5 \le \phi/\phi_0 < 0.5$,

$$I_{1}(\phi) = -I_{0} \left\{ \frac{2\phi}{\phi_{0}} - \frac{2}{\pi} \tan^{-1} \left[\frac{\epsilon \tan(\pi\phi/\phi_{0})}{2 - \epsilon - 2\sqrt{1 - \epsilon}} \right] \right\}. \tag{30}$$

with $I_0 = ev_F/L_x$. From Equation (30), we see that ϵ can vary in the range $0 \le \epsilon \le 1$; there is nothing special about $\epsilon = 1/2$, as it might have seemed from Equation (28).

The above model assumes that an inelastic event may take place only at one particular point along the ring. A more realistic model consists of coupling the ring to external reservoirs at many points along the ring, as shown in Figure 11(b). We have studied a model of a ring with infinitely many couplings to identical reservoirs uniformly spaced over the whole ring. The relevant parameter in this model is the probability that the electron not be inelastically scattered while moving through the ring once. We choose this parameter to be equal to $\exp(-L/L_{\phi})$, which is a reasonable way to define the phase-coherence length, L_{ϕ} . Assuming ballistic motion of the electron, one may alternatively set L_{ϕ} to be $v_{\rm F}\tau_{\phi}$, where τ_{ϕ} is the dephasing time. Quantummechanical coherence is lost on length scales larger than $L_{\scriptscriptstyle \phi}$. In our generalized model, the persistent current is given again by Equation (30), with $(1 - \epsilon)$ replaced by $\exp(-L/L_{\phi})$. In the limit $L_{\phi} \gg L$, the current becomes

$$I_{1}(\phi) = -I_{0} \left[\frac{2\phi}{\phi_{0}} - \frac{L}{2\pi L_{1}} \tan\left(\frac{\pi\phi}{\phi_{0}}\right) \right]; \tag{31}$$

i.e., the correction to the current is linear in L/L_{ϕ} . In the limit $L_{\phi} \ll L$, the current amplitude decreases exponentially,

$$I_1(\phi) = -\frac{2I_0}{\pi} \exp\left(-\frac{L}{2L_{\phi}}\right) \sin\left(\frac{2\pi\phi}{\phi_0}\right). \tag{32}$$

The generalization of these results to the multichannel case remains to be worked out.

5. Persistent current and elastic scattering

Any prediction of the magnitude of the persistent current amplitude for experimental systems requires a careful study of the effects of impurities. We do not discuss this point here in any depth. We do discuss briefly the effects of elastic scattering in randomly disordered systems on the persistent current at zero temperature, which can provide some useful guidelines. Our model is the tight-binding model (14) with random on-site potentials ϵ_{ij} given by independent square distributions of strength -W/2 to +W/2. The hopping matrix element V is set constant so that the disorder parameter is W/V. We have applied this model extensively to the persistent current problem in one-dimensional loops [12] and multichannel cylinders [16].

The question is again that of the scale over which the current amplitude decays. We briefly consider the weak and strong disorder limit. We also discuss some numerical results and point out the general features.

Perturbation theory is adequate when the shifts in energy due to disorder are small compared to the level spacing. From this viewpoint, the energy parameter that determines the sensitivity of the persistent current to disorder is the level spacing, Δ_{M} . Consider the level diagrams of Figure 2. In the presence of disorder, gaps open at the points of intersection and the eigenenergies, as a function of the flux ϕ , flatten out. This means that the system is less sensitive to changes in flux. Hence, the amplitude of the persistent current is reduced, while its overall flux periodicity is preserved. Perturbation theory implies, for weak arbitrary impurity potentials, the following result. The leading correction to the current is second-order in the impurity potential, i.e., proportional to $(W/V)^2$, since the correction to the wavefunction is first-order in the impurity potential and the current operator is diagonal in the unperturbed basis. Certainly for M-channel systems, the perturbation regime is not accessible experimentally because of the generally small value of Δ_{M} .

Disorder introduces new length scales into the problem. In one- and two-dimensional disordered systems, all electron eigenstates are exponentially localized [17]. We denote the localization length of the system by ξ . For the ring geometries, we define the crossover to the strongly disordered or strongly localized regime by the condition $L_x \approx \xi$. It is clear that in the localized regime the persistent current will be exponentially small. The physical reason is that then the effect of the magnetic flux, which enters in our

approach via the phase-shifted boundary condition (1), is felt by the localized electron only as an exponentially small perturbation. We found from model calculation that in the strongly localized regime the amplitude of the persistent current does decrease exponentially with L_{ν}/ξ [12, 16].

We conclude by presenting some numerical results for persistent currents in disordered rings. The results serve to give some feeling for the crossover phenomena that occur, while at the same time demonstrating interesting similarities between the sensitivity of persistent currents to temperature and disorder, respectively.

First, we consider the case of a one-dimensional loop. Figure 12 shows numerical results for the typical persistent current $I_1(\phi)/I_0$ versus ϕ/ϕ_0 for four values of the disorder parameter W/V, as obtained for a small ring of N = 20 with 10 electrons. [These data were obtained by numerical diagonalization of the Hamiltonian (14) for one realization of disorder for each value of W/V.] Even though the simulation was performed for a very small sample, the result is generic for a one-dimensional loop. We note that the decay of the current amplitude as a function of disorder in Figure 12 is very similar to the one as a function of temperature in Figure 8. Here the persistent current approaches sinusoidal behavior for large disorder. The crossover to the strongly localized regime, $\xi < L_x$, occurs at about $W/V \approx \sqrt{105/L_x}$ [17]. Analytically, we found [12] in the limit of strong disorder (i.e., $\xi_1 < L_x$) the average persistent current

$$\overline{I}_{1}(\phi) \approx \frac{I_{0}}{2} \sin\left(\frac{2\pi\phi}{\phi_{0}}\right) \exp\left(-\frac{L_{x}}{\xi_{1}}\right),$$
 (33)

with the higher harmonics decaying with correspondingly higher powers of the exponential factor. The current \overline{I}_1 in Equation (33) is defined as the exponential of the average of $\log(I_1)$ over impurity configurations. Note that in the limit of strong disorder, $\overline{I}_1(\phi) \propto \sqrt{G}$, where G is the conductance of the ring.

Second, for the M-channel system Figure 13 exhibits the typical persistent current $I_M(\phi)/I_0$ versus ϕ/ϕ_0 for four values of the disorder parameter W/V. The results are for a small cylinder of N=8, M=4, and $\mu=0$, and were obtained by the same procedure as in the one-dimensional case. Again, though the simulation is for a very small sample, it shows generic features such as the amplitude reduction and approach to sinusoidal behavior in complete analogy to the changes occurring as a function of temperature [cf. Figures 8 and 9]. For details we refer the reader to a separate publication [16]. These analogies also suggest that to observe the persistent current does not require prohibitively small impurity concentrations.

6. Conclusion

In this paper we have addressed the question of how persistent currents in nonsuperconducting rings threaded by

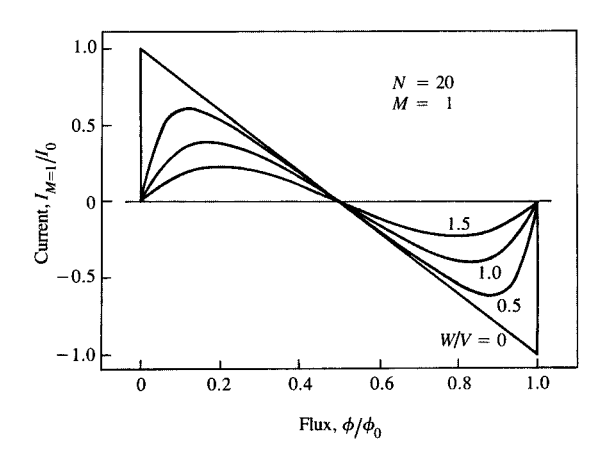


Figure 12.

Effect of disorder on the $I-\phi$ characteristics of one-channel loops from the tight-binding model. The simulation is for a small loop of N=20 with ten electrons and four values of the disorder parameter, W/V=0,0.5,1.0, and 1.5. The curves resemble those of Figure 8. See Section 5 for details.

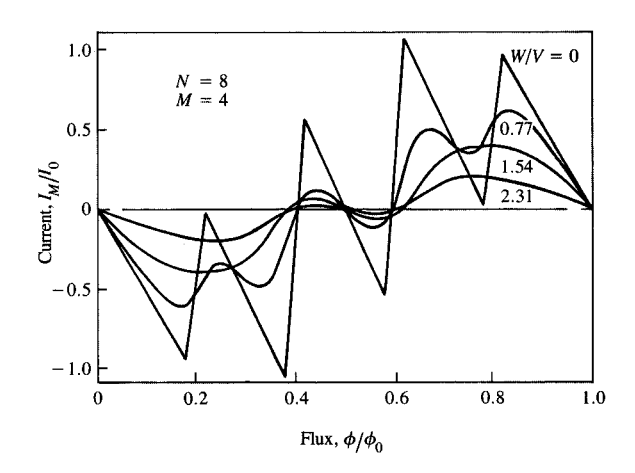


Figure 18

Effect of disorder on the $I-\phi$ characteristics of M-channel cylinders from the tight-binding model. The simulation is for a small cylinder of dimensions 8 × 4 and 16 electrons for four values of the disorder parameter, W/V = 0, 0.77, 1.54, and 2.31. The first harmonic dominates at large disorder.

a magnetic flux depend on several important physical parameters. These include the number of channels (geometry), temperature, and disorder. We have also considered the effect of inelastic scattering in the singlechannel case. The situation is much more favorable than might have been thought. Although it is too early at this stage to predict the actual magnitude of the persistent currents in experimental systems, we believe that our work has already shown that nonnegligible persistent currents should occur in isolated rings of mesoscopic dimensions. The sensitivity of these currents to material parameters might make them an interesting tool for characterizing such systems.

We emphasize that the currents are in fact rapidly fluctuating in time, due to coupling to other degrees of freedom such as phonons. The term "persistent current" refers to the nonvanishing dc component of that current. In the Introduction we stated the assumptions of our calculations. We stress that we choose to discuss the persistent-current behavior due to a pure Aharonov-Bohm effect; we ignored spin-orbit coupling and neglected further attenuation of the current due to the field penetrating through the metal. One can estimate that these assumptions pose no serious problems for appropriate ring geometries.

In Section 2, we found that in spite of massive cancellations of the currents between individual channels (and, of course, between energy levels within channels) the total current increases with the number of channels as $\sqrt{M}I_0$ for short cylinders and as $(M/\sqrt{L})I_0$ for long cylinders, where I_0 is the typical current of a single-channel ring. For special geometries one can achieve maximal phase correlation and much larger currents, $I_{\max} \propto MI_0$. Those latter cases may not be of great experimental relevance at this stage. They are of interest to the theorist since they allow the modeling of samples with specific properties, e.g., persistent currents with dominating higher harmonics.

In Section 3, we found that even for multichannel rings the sensitivity of the persistent current to temperature is governed by the characteristic energy $k_{\rm B}T^* \propto \Delta_1$, rather than the much smaller $\Delta_M \propto \Delta_1/M$. That is a somewhat surprising result in view of the fact that it is the level spacing that governs the temperature attenuation of the persistent current in the single-channel case. The explanation is, however, simple. Whereas in one dimension the ladder of states at any fixed flux yields contributions to the total current which alternate in sign, this is not the case for a higher-dimensional system. Correlations exist among the slopes of the eigenenergies as function of flux. While for one dimension the current of the last occupied level (for T = 0) gives the sign and order of magnitude of the total current, in two dimensions the total current is well represented in many cases by the contributions of levels within an energy interval of width $\Delta_1/2$ just below the Fermi energy. We shall quantify these remarks in a forthcoming publication.

In Section 4, we commented on the role of inelastic, i.e., phase-breaking, interactions. For a single-channel loop in the ballistic regime, the current is attenuated by an exponential

factor, $\exp(-L_x/L_\phi)$, that contains the phase-breaking length (or time). Theoretical questions remain to be worked out, including the dependence of the phase-breaking time on elastic scattering and the form of the attenuation of the current for the multichannel case, especially in the diffusive regime. The successful magnetoresistance experiments [3] show that it is possible to fabricate multichannel rings that possess sufficiently large phase-coherence lengths at experimentally accessible temperatures.

In Section 5, we discussed the attenuation of the persistent current due to random disorder in the system. We considered the randomly disordered tight-binding model. For realistic M-channel systems, the ballistic regime, let alone the perturbative regime, is not experimentally accessible at present. Analogies between the sensitivity of the persistent-current amplitude to temperature and degree of disorder seem to suggest that one does not require prohibitively pure samples to observe the persistent current. For small disorder in the perturbative regime, the corrections to the current are quadratic in the degree of disorder, $(W/V)^2$. For large disorder in the strongly localized regime, the persistent current amplitude is attenuated by an exponential, $\exp(-L_x/\xi)$, which contains the localization length. This is because the wavefunction reaches around the ring only via exponentially small tails; hence, its sensitivity to the Aharonov-Bohm flux (boundary conditions) is also exponentially small. We are currently working out the details of the behavior of the persistent current amplitude in the experimentally interesting intermediate regime, the diffusive regime.

Acknowledgments

We have benefitted from discussions with many colleagues, including M. Y. Azbel, M. Büttiker, Y. Imry, R. Landauer, M. Schick, W. H. Shih, D. J. Thouless, and R. A. Webb. W. H. Shih collaborated in the early stages of this project. Y. G. acknowledges with thanks the hospitality of E. K. Riedel and D. J. Thouless at the University of Washington, and also acknowledges support by the U.S.-Israel Binational Science Foundation. This work was supported in part by the National Science Foundation under Grant No. DMR85-09392.

References and notes

- Y. Imry, "Physics of Mesoscopic Systems," Directions in Condensed Matter Physics, G. Grinstein and G. Mazenko, Eds., World Scientific Press, Singapore, 1986, p. 101.
- S. Washburn and R. A. Webb, "Aharonov-Bohm Effect in Normal Metal Quantum Coherence and Transport," Adv. Phys. 35, 375 (1986).
- 3. See [2], and references therein.
- M. Büttiker, Y. Imry, and R. Landauer, "Josephson Behavior in Small Normal One-Dimensional Rings," *Phys. Lett.* 96A, 365 (1983).
- M. Büttiker, "Small Normal-Metal Loop Coupled to an Electron Reservoir," Phys. Rev. B 32, 1846 (1985); see also M. Büttiker, "Flux Sensitive Effect in Normal Metal Loops," New Techniques

- and Ideas in Quantum Measurement Theory, D. M. Greenberger, Ed., Ann. N.Y. Acad. Sci. 480, 194 (1986), and references therein.
- N. Byers and C. N. Yang, "Theoretical Considerations Concerning Quantized Magnetic Flux in Superconductor Cylinders," Phys. Rev. Lett. 7, 46 (1961).
- F. Bloch, "Off-Diagonal Long Range Order and Persistent Currents in a Hollow Cylinder," *Phys. Rev.* 137, A787 (1965); F. Bloch, "Flux Quantization and Dimensionality," *Phys. Rev.* 166, 415 (1968).
- R. Landauer, "Comments on Molecular Josephson Tunneling," Internal memo, IBM Thomas J. Watson Research Center, Yorktown Heights, NY, 1966.
- M. Schick, "Flux Quantization in a One-Dimensional Model," Phys. Rev. 166, 401 (1968).
- L. Gunther and Y. Imry, "Flux Quantization Without Off-Diagonal Long Range Order in a Thin Hollow Cylinder," Solid State Commun. 7, 1391 (1969); Y. Imry and L. Gunther (1969), unpublished (Y. Imry, Department of Nuclear Physics, The Weizmann Institute of Science, Rehovot 76 100, Israel).
- F. Bloch, "Josephson Effect in a Superconductor Ring," Phys. Rev. B 2, 109 (1970).
- H. F. Cheung, Y. Gefen, E. K. Riedel, and W. H. Shih, "Persistent Currents in Small One-Dimensional Metal Rings," Phys. Rev. B 37 (1988); for a preliminary report, see H. F. Cheung, Y. Gefen, E. K. Riedel, and W. H. Shih, "Persistent Currents in Small Metal Rings," Bull. Amer. Phys. Soc. 32, 920 (1987).
- We thank Dr. R. A. Webb for providing us with information on relevant experimental parameters.
- 14. The $I-\phi$ characteristics in this and other graphs were generated numerically by considering finite size samples and summing over all currents $I_{m,n}$ of eigenstates with energies $E_{m,n} \leq \mu$ [cf. Equations (3) and (4)], rather than from the corresponding analytical formulas. (The latter are identified in the figure captions for reference only.) Sample sizes are often not specified when the results are general.
- M. Büttiker, Y. Imry, and M. Y. Azbel, "Quantum Oscillations in One-Dimensional Normal-Metal Rings," *Phys. Rev. A* 30, 1982 (1984).
- H. F. Cheung, Y. Gefen, and E. K. Riedel (1988), unpublished manuscript; available from E. K. Riedel, Department of Physics, University of Washington, Seattle, WA 98195.
- For a review, see D. J. Thouless, "Introduction to Disordered Systems," Critical Phenomena, Random Systems, Gauge Theories, Les Houches, Session XLIII, 1984, K. Osterwalder and R. Stora, Eds., Elsevier, Amsterdam, 1986, p. 681; P. A. Lee and T. V. Ramakrishnan, "Disordered Electronic Systems," Rev. Mod. Phys. 57, 287 (1985); and A. G. Aronov and Yu. V. Sharvin, "Magnetic Flux Effects in Disordered Conductors," Rev. Mod. Phys. 59, 755 (1987).
- M. Kappus and F. J. Wegner, "Anomaly in the Band Centre of the One-Dimensional Anderson Model," Z. Phys. B 45, 15 (1981).

Received November 13, 1987; accepted for publication December 7, 1987 Ho-Fai Cheung University of Washington, Department of Physics FM-15, Seattle, Washington 98195. Dr. Cheung received his B.Sc. in physics from the University of Hong Kong in 1980, his M.S. from the University of California at Los Angeles in 1981, and his Ph.D. from the University of Illinois at Urbana-Champaign in 1986. He is currently a research associate at the University of Washington. Dr. Cheung's research interests are in the area of properties of disordered materials.

Yuval Gefen Department of Nuclear Physics, The Weizmann Institute of Science, Rehovot 76 100, Israel. Dr. Gefen is conducting research in quantum transport in ultrasmall structures. He completed his Ph.D. thesis on fractals, percolation, and localization at Tel-Aviv University in 1983, and worked as a research associate in the Institute for Theoretical Physics, University of California, Santa Barbara, and the University of Washington, Seattle. Dr. Gefen is an Alon Fellow and a Bat-Sheva de Rothschild Fellow. He is a frequent visitor to the IBM Thomas J. Watson Research Center, Yorktown Heights, New York.

Eberhard K. Riedel University of Washington, Department of Physics FM-15, Seattle, Washington 98195. Professor Riedel received his Diploma in physics from the Universität Köln, Federal Republic of Germany, in 1964 and his Dr.rer.nat. from the Technische Universität München, Federal Republic of Germany, in 1966. He worked as a research associate at the Max-Planck Institut für Physik in Munich, the Institute Laue-Langevin in Munich/ Grenoble, and Cornell University, Ithaca, New York. From 1971–1975 he taught at Duke University, Durham, North Carolina; he is now a professor of physics at the University of Washington. In 1978, he was a NORDITA Professor at the Niels Bohr Institute in Copenhagen. Professor Riedel is a Fellow of the American Physical Society. His research interests are in the areas of physics of mesoscopic systems and phase transitions and critical phenomena.